Effect of the Solvent on the Crystallographic and Magnetic Properties of rhenium(IV) Complexes Based on 2,2′-Bipyrimidine Ligand

Adrián Sanchis-Perucho , Marta Orts-Arroyo , Nicolas Moliner , José Martínez-Lillo *

Posted Date: 2 February 2023

doi: 10.20944/preprints202302.0036.v1

Keywords: rhenium; 2,2'-bipyrimidine; metal complexes; crystal structure; crystal explorer; magnetic properties

Article

Effect of the Solvent on the Crystallographic and Magnetic Properties of Rhenium(IV) Complexes Based on 2,2′-Bipyrimidine Ligand

Adrián Sanchis-Perucho, Marta Orts-Arroyo, Nicolas Moliner and José Martínez-Lillo *

Departament de Química Inorgànica/Instituto de Ciencia Molecular (ICMol), Universitat de València, c/Catedrático José Beltrán 2, Paterna, 46980 València, Spain; adrián.sanchis@uv.es (A.S.-P.); marta.orts-arroyo@uv.es (M.O.-A.); fernando.moliner@uv.es (N.M.)

* Correspondence: f.jose.martinez@uv.es; Tel.: +34-9635-44460

Abstract: Two solvated rhenium(IV) complexes with formula $[ReCl_4(bpym)]\cdot MeCN$ (**1**) and $[ReCl_4(bpym)]\cdot CH_3COOH\cdot H_2O$ (**2**) [bpym = 2,2′-bipyrimidine] have been prepared and characterized by means of Fourier transform infrared spectroscopy (FT–IR), scanning electron microscopy and energy dispersive X-ray analysis (SEM–EDX), single-crystal X-ray diffraction (XRD) and SQUID magnetometer. **1** and **2** crystallize in the monoclinic system with space groups $P2_1/n$ and $P2_1/c$, respectively. In both compounds, the Re(IV) ion is six-coordinate and bound to four chloride ions and two nitrogen atoms of a 2,2′-bipyrimidine molecule forming a distorted octahedral geometry around the metal ion. In the crystal packing of **1** and **2**, intermolecular halogen···halogen and π···halogen type interactions are present. Hydrogen bonds take place only in the crystal structure of **2**. Both compounds exhibit an akin crystal framework based on halogen bonds. Variable-temperature dc magnetic susceptibility measurements performed on microcrystalline samples of **1** and **2** show a similar magnetic behavior for both compounds, with antiferromagnetic exchange between the Re(IV) ions connected mainly through intermolecular Re-Cl···Cl-Re interactions.

Keywords: rhenium; 2,2′-bipyrimidine; metal complexes; crystal structure; crystal explorer; magnetic properties

1. Introduction

The study on solvate formation in crystalline compounds is becoming increasingly a significant topic, given the academic and industrial interest in elucidating the properties and variations in morphology of different crystal forms [1,2]. Many times the crystallization solvent can explain the observed changes in physical properties of a crystalline material, and this investigation can assist in the ongoing efforts to improve the design of crystallization processes from solution [1–5].

In the coordination chemistry of Re(IV), the polymophism and the effect of the solvent on the magnetic properties of Re(IV) complexes have been relatively little studied [6,7]. The mononuclear complexes based on halides of Re(IV) ion have been investigated during decades and are characterized by large values of magnetic anisotropy and significant intermolecular magnetic exchange [8–22]. Indeed, these compounds can display relatively strong dipolar exchange through Re–X···X–Re type contacts (X = halogen), which can result in a magnetic order as, for instance, metamagnetism or spin canting [23–25].

The neutral mononuclear $[ReCl_4(bpym)]$ complex has been previously studied, showing remarkable properties [26]. It displays potent in vitro anti-proliferative activity against a series of cancer cells [27]. Regarding its magnetic properties, it exhibits magnetic ordering below 7.0 K through the spin-canting phenomenon, with values of the coercive field (Hc) and remanent magnetization (Mr) of 1750 G and 0.05 μB, respectively [28]. Besides, it has been employed as starting material for

Preprints (www.preprints.org) | NOT PEER-REVIEWED | Posted: 2 February 2023 doi:10.20944/preprints202302.0036.v1

the preparation of rhenium-based compounds as, for instance, the first heterodinuclear 2,2′-bipyrimidine-bridged complex magnetostructurally studied, of the formula $[ReCl_4(\mu\text{-}bpym)NiBr_2(H_2O)_2]$ [29], and the chiral, photoluminescent, and spin-canted compound of formula $\{CuReCl_4(\mu\text{-}Cl)(\mu\text{-}pyz)[ReCl_4(\mu\text{-}bpym)]\}\cdot MeNO_2$ [30]. More recently, two one-dimensional coordination polymers of general formula $\{[ReCl_4(\mu\text{-}bpym)CuX_2]\cdot solvent\}_n$ have been characterized structurally and magnetically [31].

To develop our investigation on the effect of the solvent and the intermolecular interactions on the magnetic properties of Re(IV) compounds, we herein report the synthesis, crystal structure and magnetic properties of two solvated Re(IV) complexes based on the 2,2′-bipyrimidine ligand, with formula $[ReCl_4(bpym)]\cdot MeCN$ (**1**) and $[ReCl_4(bpym)]\cdot CH_3COOH\cdot H_2O$ (**2**), which are compared with the unsolvated complex.

2. Results and Discussion

2.1. Description of the crystal structures

The crystal structures of **1** and **2** were studied through the single-crystal X-ray diffraction technique. Both compounds crystallize in the monoclinic crystal system with space groups $P2_1/n$ and $P2_1/c$, respectively (Table 1). The not solvated $[ReCl_4(bpym)]$ complex crystallizes in the orthorhombic space group $P2_12_12_1$ [26]. The crystal structure of **1** is made up of neutral $[ReCl_4(bpym)]$ complexes and MeCN molecules, whereas the crystal structure of **2** is based on $[ReCl_4(bpym)]$, CH_3COOH and H_2O molecules, as showed in their respective asymmetric units (Figures 1 and 2).

In the mononuclear $[ReCl_4(bpym)]$ complexes of **1** and **2**, each Re(IV) ion is bonded to four chloride ions and two nitrogen atoms of a 2,2′-bipyrimidine molecule forming a distorted octahedral geometry around the metal ion. In both compounds, the average values of the Re–N bond lengths [2.129(1) Å for **1** and 2.137(1) Å for **2**] are shorter than those of the Re–Cl bond lengths [2.317(1) Å for **1** and 2.308(1) Å for **2**], displaying values which are in agreement with those previously published for similar Re(IV) complexes [26,32]. Besides, the Re-Cl bond lengths in axial positions are longer than those located in equatorial positions in both **1** and **2** (Figures 1 and 2). The chelating 2,2′-bipyrimidine molecule is pretty much planar in both compounds, and exhibit average C–C, N–N, and C–N bond length values in agreement with those found in similar bpym-based complexes containing 4d and 5d metal ions [33,34].

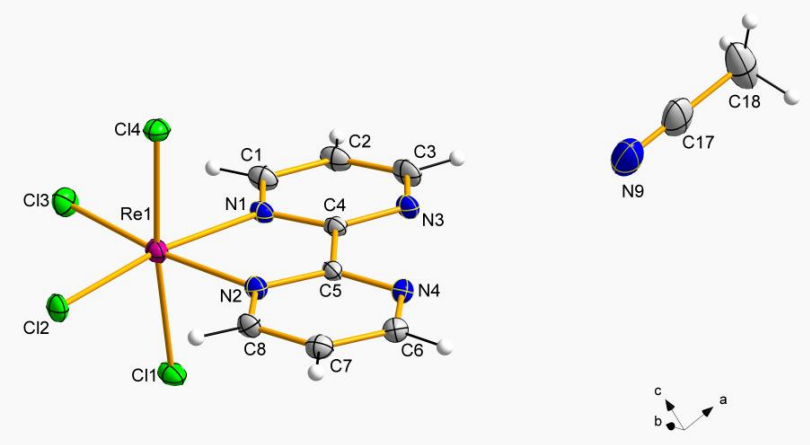

Figure 1. Detail of the mononuclear $[ReCl_4(bpym)]$ complex and solvent MeCN molecule in **1**. Thermal ellipsoids are depicted at the 50% probability level.

Preprints (www.preprints.org) | NOT PEER-REVIEWED | Posted: 2 February 2023 doi:10.20944/preprints202302.0036.v1

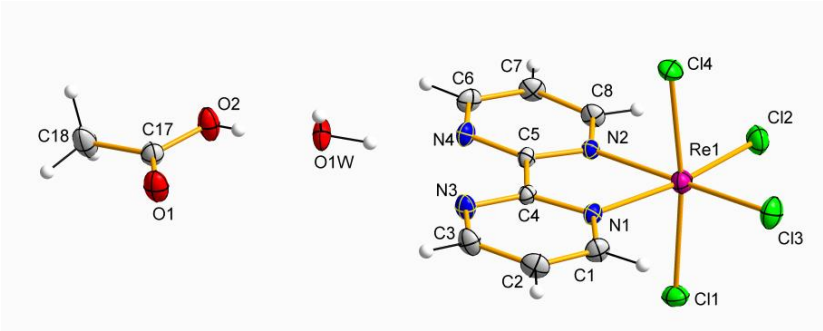

Figure 2. Detail of the mononuclear [$ReCl_4$(bpym)] complex and solvent molecules in **2**. Thermal ellipsoids are depicted at the 50% probability level.

In the crystal packing of **1**, intermolecular short Cl···Cl contacts of 3.559(1) Å [Cl(3)···Cl(7a) distance with (a) = x−1, y, z] and 3.560(1) Å [Cl(2)···Cl(6b) distance with (b) = x−1, y−1, z] direct alternate chains formed by complexes of Re(1) and Re(2) ions, which grow along the crystallographic c axis (Figure 3). These chains are interlinked with each other through C-H···N interactions involving neighboring bpym ligands [C(15c)···N(4) distance being ca. 3.50 Å; (c) = x, y−1, z], and also with somewhat longer Cl···Cl contacts of ca. 3.667(1) Å, resulting in a corrugated layered structure that grows in the ac plane (Figure 3). Further C-H···N interactions [C(6d)···N(9) distance being ca. 3.62 Å; (d) = −x+1, −y+2, −z+1] occur between [$ReCl_4$(bpym)] complexes and MeCN solvent molecules. These intermolecular interactions, along with π···Cl contacts of ca. 3.283(1) Å and several weak C-H···Cl interactions, draw together a 3D crystal structure in compound **1**.

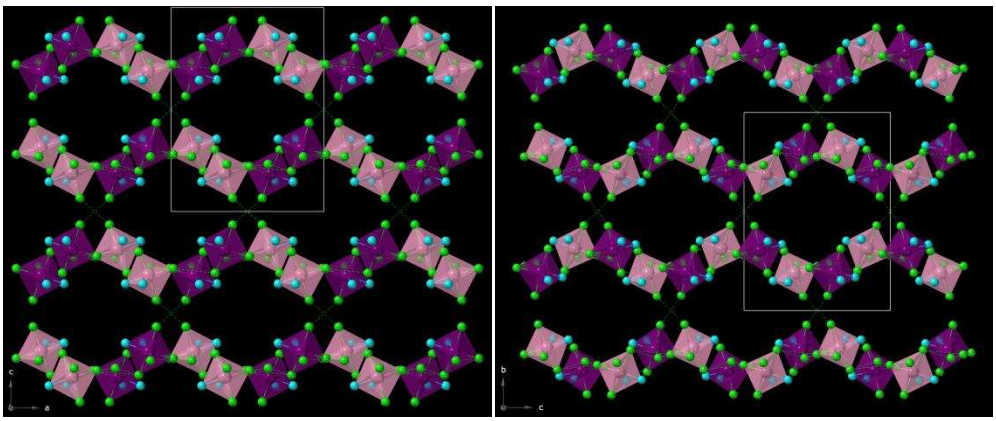

Figure 3. View along the crystallographic b axis of the one-dimensional motifs of [$ReCl_4$(bpym)] complexes (polyhedron model) connected through Cl···Cl interactions in **1** (left); View along the crystallographic a axis of the one-dimensional motifs of [$ReCl_4$(bpym)] complexes (polyhedron model) connected through Cl···Cl interactions in **2**. Solvent molecules and bpym ligand have been omitted for clarity.

In the crystal packing of **2**, several O-H···O and O-H···N hydrogen bonds connect the solvent molecules CH_3COOH and H_2O to the [$ReCl_4$(bpym)] complexes [O1w···N(7a) distance of ca. 2.866 Å; (a) = -x+1, y-1/2, -z+3/2] (Table 2). As in **1**, chains formed through alternate complexes of Re(1) and Re(2) ions are generated by short Cl···Cl contacts (Figure 3). In the case of **2**, this type of halogen···halogen bonds are shorter than those found in **1** [the shortest one being Cl(3)···Cl(7b) with distance of ca. 3.309 Å and (b) = x+1, -y+3/2, z+1/2] (Figure 3). Further Cl···Cl contacts of approximately 3.708 Å, together with C-H···N interactions between bipyrimidine rings of adjacent [$ReCl_4$(bpym)] complexes, link the chains forming 2D sheets [C(6c)···N(8) distance of ca. 3.507 Å; (c) = x, -y+3/2, z+1/2] (Figure 4).

Preprints (www.preprints.org) | NOT PEER-REVIEWED | Posted: 2 February 2023 doi:10.20944/preprints202302.0036.v1

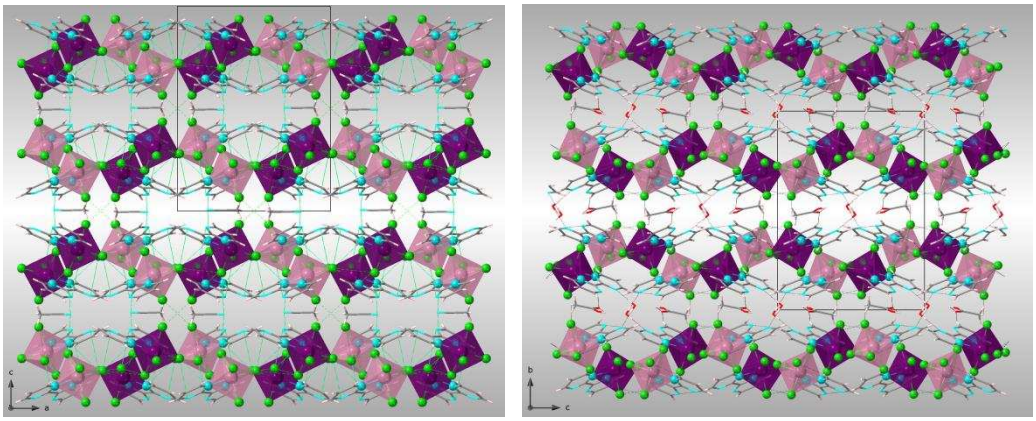

Figure 4. View along the crystallographic b axis of the intermolecular interactions between [$ReCl_4$(bpym)] complexes and between [$ReCl_4$(bpym)] complexes and MeCN molecules in **1** (left); View along the crystallographic a axis of the intermolecular interactions between [$ReCl_4$(bpym)] complexes and CH_3COOH and H_2O molecules in **2**.

Table 1. Summary of the crystal data and structure refinement parameters for **1** and **2.**

Compound	1	2
CIF	2233243	2233244
Formula	$C_{18}H_{15}Cl_8N_9Re_2$	$C_{18}H_{18}Cl_8N_8O_3Re_2$
Fw/g mol^{-1}	1013.39	1050.40
Temperature/K	120(2)	120(2)
Crystal system	monoclinic	monoclinic
Space group	$P2_1/n$	$P2_1/c$
a/Å	13.239(1)	11.960(1)
b/Å	11.852(1)	18.089(1)
c/Å	17.666(1)	13.433(1)
α/°	90	90
β/°	90.02(1)	93.02(1)
γ/°	90	90
V/Å^3	2771.97(13)	2902.30(10)
Z	4	4
D_c/g cm^{-3}	2.428	2.404
μ(Mo-K$_\alpha$)/mm^{-1}	9.526	9.110
F(000)	1888	1968
Goodness-of-fit on F^2	1.307	1.061
R_1 [$I > 2\sigma(I)$]/all data	0.0221/0.0252	0.0377/0.0424
wR_2 [$I > 2\sigma(I)$] /all data	0.0649/0.0773	0.0793/0.0816

Table 2. Selected hydrogen-bonding interactions in **2.**

D-H···A	D-H/Å	H···A/Å	D···A/Å	(DHA)/°
O(2)-H(2A)···O(1w)	0.888	1.91(1)	2.599(1)	173.6(1)
O(1w)-H(1wB)···N(4)	0.927	1.91(1)	2.804(1)	162.7(1)
O(1w)-H(1wA)···N(7a)	0.935	1.97(1)	2.866(1)	160.8(1)
O(1w)-H(1wA)···N(8a)	0.935	2.67(1)	3.301(1)	125.4(1)

In **2**, there are π···Cl contacts, involving bipyrimidine rings and chloride anions, which are of approximately 3.283(1) Å, and also weak C-H···Cl interactions, which implicate the methyl group of the CH_3COOH molecules and chloride anions of the [$ReCl_4$(bpym)] complexes [C(18)···Cl(5d)

Preprints (www.preprints.org) | NOT PEER-REVIEWED | Posted: 2 February 2023 doi:10.20944/preprints202302.0036.v1

distance of ca. 3.617 Å; (d) = x+1, -y+3/2, z-1/2]. These last intermolecular interactions also contribute to stabilizing the crystal structure in compound **2** (Figure 4).

2.2. Hirshfeld Surface Analysis

Hirshfeld surfaces of the neutral [$ReCl_4$(bpym)] complex in compounds **1** and **2** were calculated and their close intermolecular interactions were analyzed through the CrystalExplorer program [35–37]. CrystalExplorer calculates a series of surfaces which allow obtaining a both qualitative and quantitative visualization of the main intermolecular interactions, in this case, taking place in **1** and **2**, the shorter contacts being shown with red color [38,39]. This is performed by mapping the distances from the surface to the nearest atom outside (d_e) and inside (d_i) of each surface and, at the same time, considering a normalized contact distance (d_{norm}) that takes into account some limitations generated by the atomic radii [35–37]. The Hirshfeld surfaces for compounds **1** and **2** are given in Figures 5 and 6, respectively. According to their fingerprint plots, both **1** and **2** show a very similar percentage regarding the intermolecular Cl···Cl contacts between adjacent [$ReCl_4$(bpym)] complexes [ca. 6.4% for **1** and ca. 6.3% for **2**], which is consistent with the akin framework based on halogen bonds that both compounds exhibit (Figure 7). The Cl···H contacts connecting mainly chloride anions and C-H groups of neighboring [$ReCl_4$(bpym)] complexes in **1** and **2**, and also the methyl groups of CH_3COOH molecules in the case of **2**, are the main interactions observed on the Hirshfeld surfaces for both compounds, which cover ca. 34.9% for **1** and ca. 39.2% for **2** on their respective fingerprint plots (Figures 5 and 6). Finally, further N···H contacts involving solvent molecules, mainly MeCN (in **1**) and H_2O (in **2**), and N atoms and C-H groups of adjacent bipyrimidine rings are approximately 11.6% and 9.7% of the complete fingerprint plot of **1** and **2**, respectively (Figures 5 and 6).

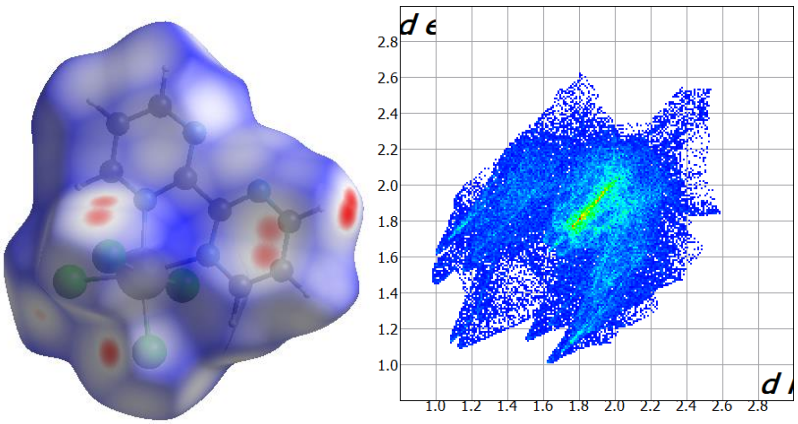

Figure 5. Hirshfeld surface mapped through d_{norm} function for **1** (left); Full fingerprint plot for the dinuclear Re(IV) compound **1** (right).

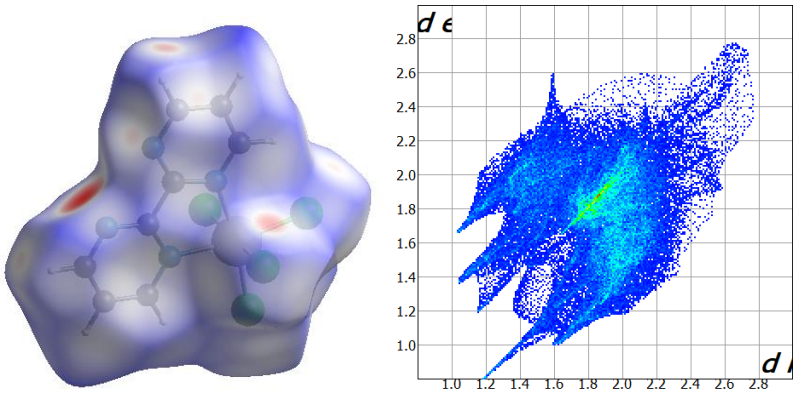

Figure 6. Hirshfeld surface mapped through d_{norm} function for **2** (left); Full fingerprint plot for the dinuclear Re(IV) compound **2** (right).

Preprints (www.preprints.org) | NOT PEER-REVIEWED | Posted: 2 February 2023 doi:10.20944/preprints202302.0036.v1

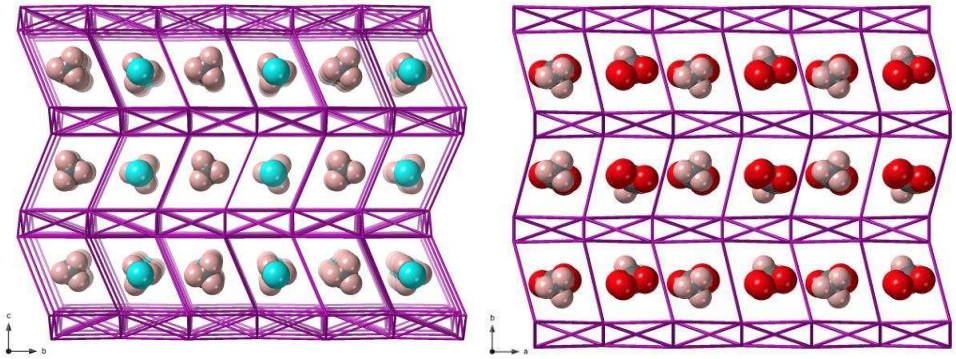

Figure 7. View along the crystallographic a axis of the grid formed by [$ReCl_4$(bpym)] complexes connected through intermolecular Cl···Cl bonds acting as host of MeCN molecules in **1** (left); View along the crystallographic c axis of the grid formed by [$ReCl_4$(bpym)] complexes connected through intermolecular Cl···Cl bonds acting as host of CH_3COOH and H_2O molecules in **2** (right).

2.3. Magnetic Properties

Dc magnetic susceptibility measurements were performed on microcrystalline samples of **1** and **2** in the 2-300 K temperature range and under an external magnetic field of 0.5 T. The resulting $\chi_M T$ *versus* T plots (χ_M being the molar magnetic susceptibility per mononuclear Re(IV) complex) for compounds **1** and **2** are shown in Figure 8. At 300 K, the $\chi_M T$ values are *ca.* 1.57 (**1**) and *ca.* 1.54 $cm^3mol^{-1}K$ (**2**), which are very close to those earlier published for magnetically isolated complexes based on Re(IV) ion ($5d^3$ ion with S = 3/2) [7]. Upon cooling, the curve that the $\chi_M T$ values draw for **1** follow the Curie law with decreasing temperature to approximately 100 K, before they decrease reaching minimum values of approximately 0.17 $cm^3mol^{-1}K$ at 2.0 K (Figure 8). In the case of **2**, the $\chi_M T$ values decrease gradually with decreasing temperature, and more abruptly at approximately 50 K, reaching a minimum value of 0.49 $cm^3mol^{-1}K$ at 2.0 K (Figure 8). The decrease of the $\chi_M T$ value observed for both **1** and **2** would be assignable to antiferromagnetic interactions as well as zero-field splitting (ZFS) effects [40,41]. No maximum of the magnetic susceptibility is observed for either compound, as shown in their respective χ_M *versus* T plots (insets in Figure 8).

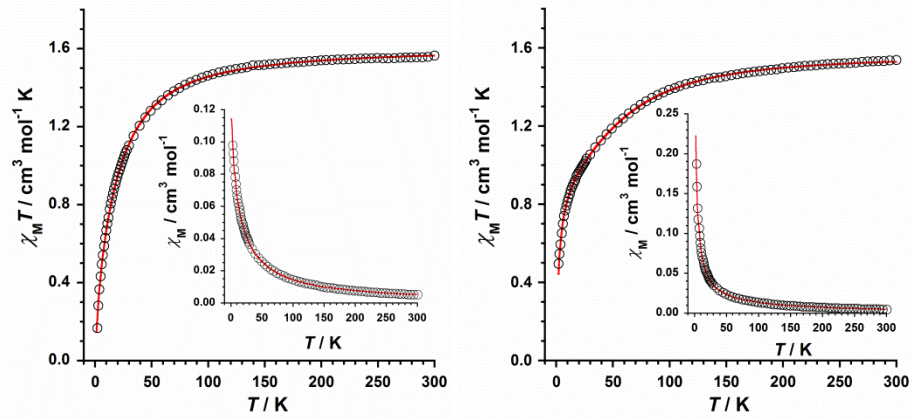

Figure 8. Thermal variation of the $\chi_M T$ product for compounds **1** (left) and **2** (right). The solid red line represents the theoretical fit of the experimental data and the inset shows the χ_M versus T plot.

As indicated in the description of the crystal structure of **1** and **2**, both compounds exhibit short Cl···Cl contacts between the paramagnetic [$ReCl_4$(bpym)] complexes in their crystal lattices (Figure 3). Hence, these relatively important through-space interactions between Re(IV) ions precludes the occurrence of SIM behavior [40,41]. Besides, the presence of solvent molecules changes drastically the magnetic properties, given that the unsolvated [$ReCl_4$(bpym)] complex exhibits magnetic ordering

Preprints (www.preprints.org) | NOT PEER-REVIEWED | Posted: 2 February 2023 doi:10.20944/preprints202302.0036.v1

through spin-canting, as previously reported [7,28], a magnetic behaviour which is not observed neither in **1** nor in **2**.

$$\hat{H} = D\left[(\hat{S}_Z)^2 - S(S+1)/3\right] + g\beta H\hat{S} \quad (1)$$

$$\chi_M = \frac{\chi_{//} + 2\chi_\perp}{3} \quad (2)$$

$$\chi_{//} = \frac{N\beta^2 g_{//}^2}{4k(T-\theta)} \frac{1+9\exp(-2D/kT)}{1+\exp(-2D/kT)}$$

$$\chi_\perp = \frac{N\beta^2 g_\perp^2}{k(T-\theta)} \frac{1+(3kT/4D)\left[1-\exp(-2D/kT)\right]}{1+\exp(-2D/kT)}$$

To analyze the magnetic behavior of **1** and **2**, we have employed the Hamiltonian of equation (1) and its derived theoretical expression for the magnetic susceptibility, equation (2), by including a θ term to account for the observed intermolecular interactions, where $\hat{S}_z$ is the easy-axis spin operator, H is the applied field, β is the Bohr magneton, the g parameter is the Landé factor and D is the zero-field splitting (ZFS) for the Re(IV) ion [7]. Thus, the first term in equation (1) corresponds to the ZFS and the second term to the Zeeman effects. Besides, we have assumed that $g_{||} = g_\perp = g$ for complexes **1** and **2**. The best least-squares fit gave the parameters D = 31.9 cm^{-1}, g = 1.86, θ = -5.3 K and R = 2.94·10^{-5} for **1** and D = 35.8 cm^{-1}, g = 1.83, θ = - 8.8 K and R = 4.52·10^{-5} for **2** {R being the agreement factor defined as $\Sigma_i[(\chi_M T)_i^{obs} - (\chi_M T)_i^{calcd}]^2/[(\chi_M T)_i^{obs}]^2$}. As shown in Figure 8, the calculated curves (solid red lines) reproduce quite well the experimental magnetic data in the whole temperature range. The D and g values calculated for **1** and **2** are in agreement with those earlier reported for mononuclear Re(IV) complexes [7,8]. The sign and magnitude of the θ values corroborate the presence of relatively strong antiferromagnetic exchanges between the Re(IV) ions connected through intermolecular Re-Cl···Cl-Re pathways (Figure 3), with the shorter interactions in **2** [ca. 3.6 Å (in **1**) *versus* ca. 3.3 Å (in **2**)] resulting in stronger antiferromagnetic exchange.

3. Experimental Section

3.1. Materials

All manipulations were performed under aerobic conditions, using all the solvents and chemicals as received. The Re(IV) precursors, [ReCl$_4$(bpym)] [26] and (NBu$_4$)$_2$[ReCl$_4$(ox)] [42], were prepared following literature procedures.

3.2. Preparation of the complexes

3.2.1. Synthesis of [ReCl$_4$(bpym)]·MeCN (1)

1 was prepared by dissolving [ReCl$_4$(bpym)] (0.05 mmol, 24.3 mg) in 2 mL of a N,N-dimethylformamide-acetonitrile (1:1, v/v) mixture, followed by a slow diffusion in isopropanol at room temperature. Brown crystals of **1** were thus obtained in a few days and were suitable for single-crystal X-ray diffraction studies. Yield: ca. 75%. Anal. Calcd. for C$_{10}$H$_9$N$_5$Cl$_4$Re (**1**): C, 9.5; H, 3.2; N, 5.5. Found: C, 9.9; H, 3.0; N, 5.3. SEM-EDAX: a molar ratio of 1:4 for Re/Cl was found for **1**. IR (KBr pellet) peaks are observed at 3100 (m), 3067 (s), 2245 (m), 1578 (vs), 1541 (m), 1453 (w), 1407 (vs), 1269 (w), 1213 (m), 1113 (m), 1021 (s), 987 (w), 818 (m), 747 (s), 693 (m), 665 (s), 490 (w), 440 (w) cm^{-1}.

Preprints (www.preprints.org) | NOT PEER-REVIEWED | Posted: 2 February 2023 doi:10.20944/preprints202302.0036.v1

3.2.2. Synthesis of $[ReCl_4(bpym)]\cdot CH_3COOH\cdot H_2O$ (2)

2 was prepared through ligand substitution of the previously reported $(NBu_4)_2[ReCl_4(ox)]$ complex. $(NBu_4)_2[ReCl_4(ox)]$ (0.12 mmol, 110 mg) and 2,2′-bipyrimidine (0.25 mmol, 39.5 mg) were mixed in glacial acetic acid (4.0 mL). The mixture was heated to 100 °C and stirred for 4h. The resulting solution was filtered while hot and left to evaporate at room temperature. Dark orange crystals of **2** were grown in less than 1 week, and were suitable for X-ray diffraction data collection. Yield: ca. 60%. Anal. Calcd for $C_{10}H_{12}N_4O_3Cl_4Re$ (**2**): C, 21.3; H, 2.1; N, 9.9. Found: C, 21.4; H, 2.0; N, 9.6. SEM-EDAX: a molar ratio of 1:4 for Re/Cl was found for **2**. IR (KBr pellet) peaks are observed at 3424 (br), 3091 (m), 3066 (m), 1711 (m), 1579 (vs), 1547 (m), 1452 (w), 1436 (w), 1406 (vs), 1303 (w), 1258 (m), 1211 (w), 1109 (m), 1024 (s), 989 (w), 877 (w), 819 (m), 748 (s), 695 (m), 669 (m), 617 (w), 515 (w) cm^{-1}.

3.3. X-ray data collection and structure refinement

X-ray diffraction data collection on single crystals of dimensions 0.28 x 0.21 x 0.21 (**1**) and 0.17 x 0.16 x 0.06 mm^3 (**2**) were collected on a Bruker D8 Venture diffractometer with PHOTON II detector and by using monochromatised Mo-K_α radiation (λ = 0.71073 Å). Crystal parameters and refinement results for **1** and **2** are summarized in Table 1. The structures were solved by standard direct methods and subsequently completed by Fourier recycling using the SHELXTL [43] software packages and refined by the full-matrix least-squares refinements based on F^2 with all observed reflections. The final graphical manipulations were performed with the DIAMOND [44] and CRYSTALMAKER [45] programs. CCDC 2233243 and 2233244 for **1** and **2**, respectively.

3.4. Physical measurements

Elemental analyses (C, H, N) were performed in an Elemental Analyzer CE Instruments CHNS1100 and the molar ratio between heavier elements was found by means of a Philips XL-30 scanning electron microscope (SEM-EDAX), equipped with system of X-ray microanalysis, in the Central Service for the Support to Experimental Research (SCSIE) at the University of Valencia. Infrared spectra (IR) of **1** and **2** were recorded with a PerkinElmer Spectrum 65 FT-IR spectrometer in the 4000-400 cm^{-1} region. Variable-temperature, solid-state dc magnetic susceptibility data were collected on a Quantum Design MPMS-XL SQUID magnetometer equipped with a 5 T dc magnet. Experimental magnetic data were corrected for the diamagnetic contributions of both the sample holder and the eicosene. The diamagnetic contribution of the involved atoms was corrected by using Pascal's constants [46].

4. Conclusions

In summary, the synthesis, crystal structure and magnetic properties of two novel solvated Re(IV) complexes based on the 2,2′-bipyrimidine ligand, with formula $[ReCl_4(bpym)]\cdot MeCN$ (**1**) and $[ReCl_4(bpym)]\cdot CH_3COOH\cdot H_2O$ (**2**), have been reported. In the crystal structures of **1** and **2**, there are present intermolecular halogen···halogen and π···halogen type interactions and only in compound **2** there exist O-H···O and O-H···N hydrogen bonds. Having into account the presence of Re-Cl···Cl-Re contacts, both compounds exhibit a corrugated crystal framework, which host the solvent molecules. The investigation of the magnetic properties of **1** and **2** through dc magnetic susceptibility measurements reveals a similar magnetic behavior, since both compounds display antiferromagnetic exchange couplings between Re(IV) ions. The magnetic properties can be drastically modified by the presence of solvent molecules, given that the unsolvated $[ReCl_4(bpym)]$ complex exhibits a very different magnetic behaviour, that is, magnetic ordering through spin-canting, as previously reported. In this way, by changing suitable solvents, it is possible to tune the magnetic properties in this type of Re(IV) complexes.

Supplementary Materials: The following supporting information can be downloaded at the website of this paper posted on Preprints.org.

Author Contributions: Conceptualization, J.M.-L.; funding acquisition, J.M.-L.; methodology, A.S.-P., M.O.-A., N.M. and J.M.-L.; investigation, A.S.-P., M.O.-A., N.M. and J.M.-L.; formal analysis, A.S.-P., M.O.-A., N.M. and J.M.-L.; writing-original draft preparation, J.M.-L.; writing-review and editing, J.M.-L. All authors have read and agreed to the published version of the manuscript.

Funding: This research was funded by Spanish Ministry of Science and Innovation [Grant numbers PID2019-109735GB-I00 and CEX2019-000919-M (Excellence Unit "María de Maeztu")].

Data Availability Statement: The raw data that support the findings of this study are available from the corresponding author upon reasonable request.

Acknowledgments: A.S.-P. and M.O.-A. thank the Spanish "FPU fellowships" and "FPI fellowships" programs, respectively.

Conflicts of Interest: The authors declare no conflict of interest.

References

1. Price, C.P.; Glick, G.D.; Matzger, A.J. Dissecting the Behavior of a Promiscuous Solvate Former. *Angew. Chem., Int. Ed*. **2006**, *45*, 2062-2066,
2. Shan, N.; Zaworotko, M.J. The role of cocrystals in pharmaceutical science. *Drug Discov*. **2008**, *13*, 440-446.
3. Cruz-Cabeza, A.J.; Reutzel-Edens, S.M.; Bernstein, J. Facts and fictions about polymorphism. *Chem. Soc. Rev*. **2015**, *44*, 8619-8635.
4. Takieddin, K.; Khimyak, Y. Z.; Fábián, L. Prediction of Hydrate and Solvate Formation Using Statistical Models. *Cryst. Growth Des*. **2016**, *16*, 70-81
5. Braga, D.; Casali, L.; Grepioni, F. The Relevance of Crystal Forms in the Pharmaceutical Field: Sword of Damocles or Innovation Tools?. *Int. J. Mol. Sci*. **2022**, *23*, 9013.
6. Martínez-Lillo, J.; Armentano, D.; Mastropietro, T.F.; Julve, M.; Faus, J.; De Munno, G. Self-Assembled One- and Two-Dimensional Networks Based on $NH_2Me_2[ReX_5(DMF)]$ (X = Cl and Br) Species: Polymorphism and Supramolecular Isomerism in Re(IV) Compounds. *Cryst. Growth Des*. **2011**, *11*, 1733-1741.
7. Martínez-Lillo, J.; Faus, J.; Lloret, F.; Julve, J. Towards multifunctional magnetic systems through molecular-programmed self assembly of Re(IV) metalloligands. *Coord. Chem. Rev*. **2015**, *289–290*, 215-237.
8. Woodall, Ch.H.; Craig, G.A.; Prescimone, A.; Misek, M.; Cano, J.; Faus, J.; Probert, M.R.; Parsons, S.; Moggach, S.; Martínez-Lillo, J.; Murrie, M.; Kamenev, K.V.; Brechin, E.K. Pressure induced enhancement of the magnetic ordering temperature in rhenium(IV) monomers. *Nat. Commun*. **2016**, *7*, 13870.
9. González, R.; Chiozzone, R.; Kremer, C.; Guerra, F.; De Munno, G.; Lloret, F.; Julve, M.; Faus, J. Magnetic Studies on Hexahalorhenate(IV) Salts of Ferrocenium Cations $[Fe(C_5R_5)_2]_2[ReX_6]$ (R = H, CH_3; X = Cl, Br, I). *Inorg. Chem*. **2004**, *43*, 3013-3019.
10. Nelson, C.M.; Boyd, G.E.; Smith, W.T. Magnetochemistry of Technetium and Rhenium. *J. Am. Chem. Soc*. **1954**, *76*, 348-352.
11. Figgis, B.N.; Lewis, J.; Mabbs, F.E. The Magnetic Properties of Some d^3-Complexes. *J. Chem. Soc*. **1961**, 3138-3145.
12. Busey, R.; Sonder, E. Magnetic Susceptibility of Potassium Hexachlororhenate (IV) and Potassium Hexabromorhenate (IV) from 5° to 300° K. *J. Chem. Phys*. **1962**, *36*, 93-97.
13. Rouschias, G.; Wilkinson , G. The chemistry of rhenium–nitrile complexes. *J. Chem. Soc. A* **1968**, 489-496.
14. Mroziński, J. Magnetic properties of methylammonium hexachlororhenate (4) salts in the range 1.5-300 K. *Bull. Pol. Acad. Sci. Chem*. **1978**, *26*, 789-798.
15. Mroziński, J. Low temperature magnetic properties of some methylammonium hexabromorhenate (4) salts. *Bull. Pol. Acad. Sci. Chem*. **1980**, *28*, 559-567.
16. Reynolds, P.A.; Moubaraki, B.; Murray, K.S.; Cable, J.W.; Engelhardt, L.M.; Figgis, B.N. Metamagnetism in tetrachlorobis(N-phenylacetamidine)rhenium(IV). *J. Chem. Soc., Dalton Trans*. **1997**, 263-268.
17. Małecka, J.; Jäger, L.; Wagner, C.; Mroziński, J. Preparation, crystal structure and properties of $(Ph_4P)_2ReCl_6{\cdot}2CH_3CN$. *Pol. J. Chem*. **1998**, *72*, 1879-1885.
18. Reynolds, P.A.; Figgis, B.N.; Martin y Marero, D. *J. Chem. Soc., Dalton Trans*. **1999**, 945-950.
19. Thornton, P. 13 Manganese, technetium and rhenium. *Annu. Rep. Prog. Chem., Sect. A: Inorg. Chem*. **2000**, *96*, 215-228.
20. Coronado, E.; Day, P. Magnetic Molecular Conductors. *Chem. Rev*. **2004**, *104*, 5419-5448.

21. Feng, X.; Liu, J.-L.; Pedersen, K.S.; Nehrkorn, J.; Schnegg, A.; Holldack, K.; Bendix, J.; Sigrist, M.; Mutka, H.; Samohvalov, D.; et al. Multifaceted magnetization dynamics in the mononuclear complex $[Re^{IV}Cl_4(CN)_2]^{2-}$. *Chem. Commun*. **2016**, *52*, 12905–12908.
22. Pedersen, K.S.; Sigrist, M.; Sørensen, M.A.; Barra, A.-L.; Weyhermüller, T.; Piligkos, S.; Thuesen, C.Aa.; Vinum, M.G.; Mutka, H.; Weihe, H.; Clérac, R.; Bendix, J. $[ReF_6]^{2-}$: A Robust Module for the Design of Molecule-Based Magnetic Materials. *Angew. Chem. Int. Ed*. **2014**, *53*, 1351-1354.
23. González, R.; Chiozzone, R.; Kremer, C.; De Munno, G.; Nicolò, F.; Lloret, F.; Julve, M.; Faus, J. Magnetic Studies on Hexaiodorhenate(IV) Salts of Univalent Cations. Spin Canting and Magnetic Ordering in $K_2[ReI_6]$ with T_c = 24 K. *Inorg. Chem*. **2003**, *42*, 2512-2518.
24. Martínez-Lillo, J.; Kong, J.; Barros, W.P.; Faus, J.; Julve, M.; Brechin, E.K. Metamagnetic behaviour in a new Cu(II)Re(IV) chain based on the hexachlororhenate(IV) anion. *Chem. Commun*. **2014**, *50*, 5840-5842.
25. Louis-Jean, J.; Balasekaran, S.M.; Lawler, K.V.; Sanchis-Perucho, A.; Martínez-Lillo, J.; Smith, D.; Forster, P.M.; Salamat, A.; Poineau, F. Coexistence of metamagnetism and slow relaxation of magnetization in ammonium hexafluoridorhenate. *RSC Adv*. **2021**, *11*, 6353-6360.
26. Chiozzone, R.; González, R.; Kremer, C.; Cerdá, M.F.; Armentano, D.; De Munno, G.; Martínez-Lillo, J.; Faus, J. A novel series of rhenium-bipyrimidine complexes: synthesis, crystal structure and electrochemical properties. *Dalton Trans*. **2007**, 653–660.
27. Martínez-Lillo, J.; Mastropietro, T.F.; Lappano, R.; Madeo, A.; Alberto, M.E.; Russo, N.; Maggiolini, M.; De Munno, G. Rhenium(IV) compounds inducing apoptosis in cancer cells. *Chem. Commun*. **2011**, *47*, 5283-5285.
28. Martínez-Lillo, J.; Lloret, F.; Julve, M.; Faus, J. Spin canting in Re(IV) complexes: magnetic properties of $[ReX_4(bpym)]$ (X = Cl and Br; bpym = 2,2′-bipyrimidine). *J. Coord. Chem*. **2008**, *62*, 92-99.
29. Martínez-Lillo, J.; Armentano, D.; De Munno, G.; Cano, J.; Lloret, F.; Julve, M.; Faus, J. First Magnetostructural Study on a Heterodinuclear 2,2′-Bipyrimidine-Bridged Complex. *Inorg. Chem*. **2011**, *50*, 12405-12407.
30. Martínez-Lillo, J.; Armentano, D.; Fortea-Pérez, F.R.; Stiriba, S.E.; De Munno, G.; Lloret, F.; Julve, M.; Faus, J. A Chiral, Photoluminescent, and Spin-Canted $\{Cu^{I}Re^{IV}_2\}_n$ Branched Chain. *Inorg. Chem*. **2015**, *54*, 4594–4596.
31. Armentano, D.; Sanchis-Perucho, A.; Rojas-Dotti, C.; Martínez-Lillo, J. Halogen···halogen interactions in the self-assembly of one-dimensional 2,2′-bipyrimidine-based $Cu^{II}Re^{IV}$ systems. *CrystEngComm* **2018**, *20*, 4575-4581.
32. Martínez-Lillo, J.; Armentano, D.; De Munno, G.; Faus, J. Magneto-structural study on a series of rhenium(IV) complexes containing $biimH_2$, pyim and bipy ligands. *Polyhedron* **2008**, *27*, 1447-1454.
33. Roy, N.; Sen, U.; Moharana, P.; Babu, L.T.; Kar, B.; Vardhan, S.; Sahoo, S.K.; Bose, B.; Paira, P. 2,2′-Bipyrimidine-based luminescent Ru(II)/Ir(III)–arene monometallic and homo- and hetero-bimetallic complexes for therapy against MDA-MB-468 and caco-2 cells. *Dalton Trans*. **2021**, *50*, 11725-11729.
34. Yao, S.-Y.; Ou, Y.-L.; Ye, B.-H. Asymmetric Synthesis of Enantiomerically Pure Mono- and Binuclear Bis(cyclometalated) Iridium(III) Complexes. *Inorg. Chem*. **2016**, *55*, 6018-6026.
35. Turner, M.J.; McKinnon, J.J.; Wolff, S.K.; Grimwood, D.J.; Spackman, P.R.; Jayatilaka, D.; Spackman, M.A. CrystalExplorer 17; University of Western Australia, 2017.
36. McKinnon, J.J.; Jayatilaka, D.; Spackman, M.A. Towards quantitative analysis of intermolecular interactions with Hirshfeld surfaces. *Chem. Commun*. **2007**, 3814-3816.
37. Spackman, M.A.; Jayatilaka, D. Hirshfeld surface analysis. *CrystEngComm* **2009**, *11*, 19-32.
38. Spackman, P.R.; Turner, M.J.; McKinnon, J.J.; Wolff, S.K.; Grimwood D.J.; Jayatilaka, D.; Spackman, M.A. CrystalExplorer: a program for Hirshfeld surface analysis, visualization and quantitative analysis of molecular crystals. *J. Appl. Cryst*. **2021**, *54*, 1006-1011.
39. Li, S.; Bu, R.; Gou, R.-J.; Zhang, Ch.. Hirshfeld Surface Method and Its Application in Energetic Crystals. *Cryst. Growth Des.* **2021**, *21*, 6619-6634.
40. McAdams, S.G.; Ariciu, A.M.; Kostopoulos, A.K.; Walsh, J.P.S.; Floriana; Tuna, F. Molecular single-ion magnets based on lanthanides and actinides: Design considerations and new advances in the context of quantum technologies. *Coord. Chem. Rev*. **2017**, *346*, 216–239.
41. Zabala-Lekuona, A.; Seco, J.M.; Colacio, E. Single-Molecule Magnets: From Mn12-ac to dysprosium metallocenes, a travel in time. *Coord. Chem. Rev.* **2021**, *441*, 213984.

42. Chiozzone, R.; González, R.; Kremer, C.; De Munno, G.; Cano, J.; Lloret, F.; Julve, M.; Faus, J. Synthesis, Crystal Structure, and Magnetic Properties of Tetraphenylarsonium Tetrachloro(oxalato)rhenate(IV) and Bis(2,2′-bipyridine)tetrachloro(μ-oxalato)copper(II)rhenium(IV). *Inorg. Chem*. **1999**, *38*, 4745-4752.
43. SHELXTL-2013/4, Bruker Analytical X-ray Instruments, Madison, WI, 2013.
44. Diamond 4.5.0, Crystal Impact GbR, CRYSTAL IMPACT, 2018.
45. CrystalMaker 8.5.1, CrystalMaker Software Ltd, Oxford, England.
46. Bain, G.A.; Berry, J.F. Diamagnetic Corrections and Pascal's Constants. *J. Chem. Educ*. **2008**, *85*, 532-536.